swiss physical society

Nr. 62
Oktober 2020

SPG MITTEILUNGEN
COMMUNICATIONS DE LA SSP

AUSZUG - EXTRAIT

Progress in Physics (76)

Atomic buckling in silicene determined with sub-Ångstrom precision by atomic force microscopy

Rémy Pawlak, Ernst Meyer, University of Basel, Switzerland
Jorge Iribas Cerda, Instituto de Ciencia de Materiales de Madrid (ICMM), Madrid, Spain

This article has been downloaded from:
https://www.sps.ch/fileadmin/articles-pdf/2020/Mitteilungen_Progress_76.pdf

© see https://www.sps.ch/bottom_menu/impressum/

Progress in Physics (76)

Atomic buckling in silicene determined with sub-Ångstrom precision by atomic force microscopy

Rémy Pawlak, Ernst Meyer, University of Basel, Switzerland
Jorge Iribas Cerda, Instituto de Ciencia de Materiales de Madrid (ICMM), Madrid, Spain

Introduction

Since the first exfoliation of a single graphene layer from graphite in 2004 [1], mono-species two dimensional materials, generically termed Xenes [2] have attracted a tremendous interest leading to the synthesis of silicene [3], germanene [4], stanene [5] and many others [2, 6]. In contrast to the flat sp^2 nature of graphene, most Xenes exhibit an intrinsic buckling at the atomic scale due to their larger bond lengths which impede an efficient overlap, thus promoting a mixture of sp^2/sp^3 bondings. Rather than a drawback, this lack of flatness is recognized as an opportunity to achieve exciting quantum phases, particularly the quantum spin Hall (QSH) [7-9]. Indeed, the emergence of such topological properties in honeycomb Xene lattices depends on the strength of the spin-orbit coupling (SOC), which can be greatly enhanced using heavy elements in contrast to graphene. Atomic buckling thus becomes a pivotal parameter as it could significantly enhance the SOC by the corrugation [10]. To date, quantifying atomic buckling of X-ene lattice using diffraction techniques is severely restricted by their complex restructuring at surfaces or the presence of defects. On the other hand, height estimation using scanning probe techniques such as scanning tunneling microscopy (STM) is often hampered by the convolution of topographic and electronic features.

In the present article, we demonstrate that low-temperature atomic force microscopy with CO-terminated tips assisted by density functional theory enable an in-depth structural analysis of the various silicene structures on Ag(111). Our work published in PNAS is the result of an intense collaboration between the experimental group of Prof E. Meyer at the University of Basel and theoretical inputs from Dr. J. I. Cerda from the Instituto de Ciencia de Materiales de Madrid (ICMM). We believe that such investigation will help in foreseeing the precise structural characterization of analogous 2D materials where atomic buckling defects could lead to novel exotic properties.

Low-temperature force spectroscopy

These past decades, many Swiss Institutions such as IBM Rüschlikon, University of Basel or EMPA Dübendorf have pushed atomic force microscopy (AFM) imaging technique operated at low temperature with functionalized CO tips to unprecedented lateral resolutions, opening new avenues into the real-space characterization at surfaces of aromatic molecules [11-16] and 2D materials [17, 18]. Additionally, force spectroscopy further enables one to measure tip – sample forces [14] allowing to assess the atomic height variations [19]. In this context, AFM imaging and force spectroscopy combined with numerical calculations offer new opportunities to disentangle structural and electronic properties at the atomic level, notably in epitaxial Xenes,

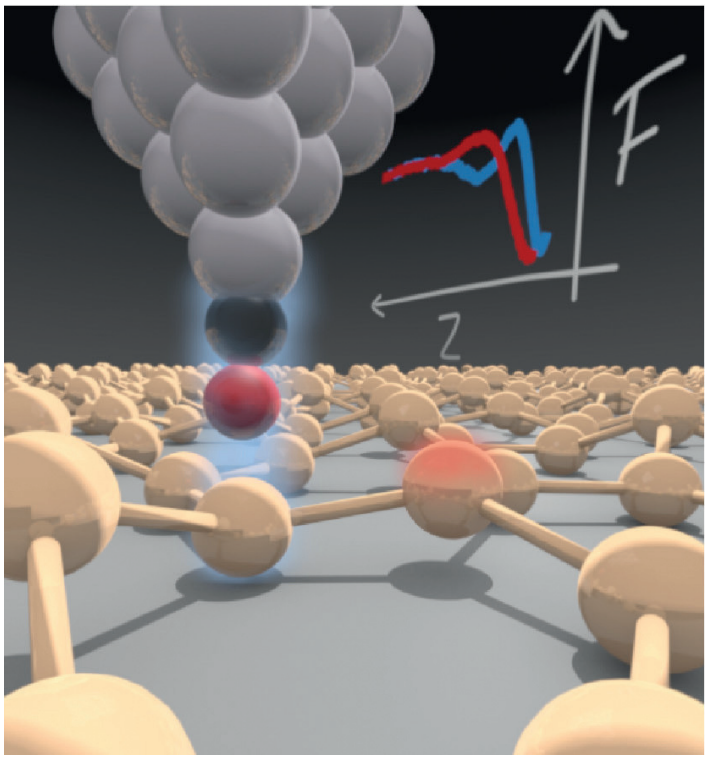

Figure 1. Artistic view of the experimental method employed to estimate the atomic buckling with sub-Ångstrom precision in silicene lattices on Ag(111). An AFM tip terminated with a single carbon monoxide (CO) molecule probes the interaction forces between tip and sample. A dip in the force-retraction curve F(Z) (background curve) is the fingerprint of the relative height of the probed atom compared to the neighboring ones (blue halo versus red halo).

specifically their intrinsic atomic buckling with sub-Ångstrom resolution.

Silicene: a paradigm of buckled Xenes

Since its first growth on Ag(111) by Vogt *et al.* in 2012 [3], the silicene properties have been widely examined using STM [3, 20-24] or angle-resolved photoemission spectroscopy (ARPES) [3, 25-27] as well as by extensive density functional theory (DFT) calculations [3, 22, 28-30]. Silicene adopts three atomically thin honeycomb structures on Ag(111) that corresponds to Si/Ag commensurate lattices: (4×4), (2√3×2√3)R30° and (√13×√13)R13.9°, denoted in the following 4×4, 2√3, and √13, respectively. The former is the most studied one and a general consensus now exists on its atomic and electronic structure [3].

To benchmark our experimental method, we first focused [31] on accurately characterizing the 4×4 phase. Figures 2A and B show experimental STM and constant-height AFM images of the 4×4 phase acquired at 4,5 K. Both images show a hexagonal arrangement of triangular patterns (dashed lines), which sides are 3,75 ± 0,05 Å. The theoretically optimized structure is displayed in Figure 1C. The most

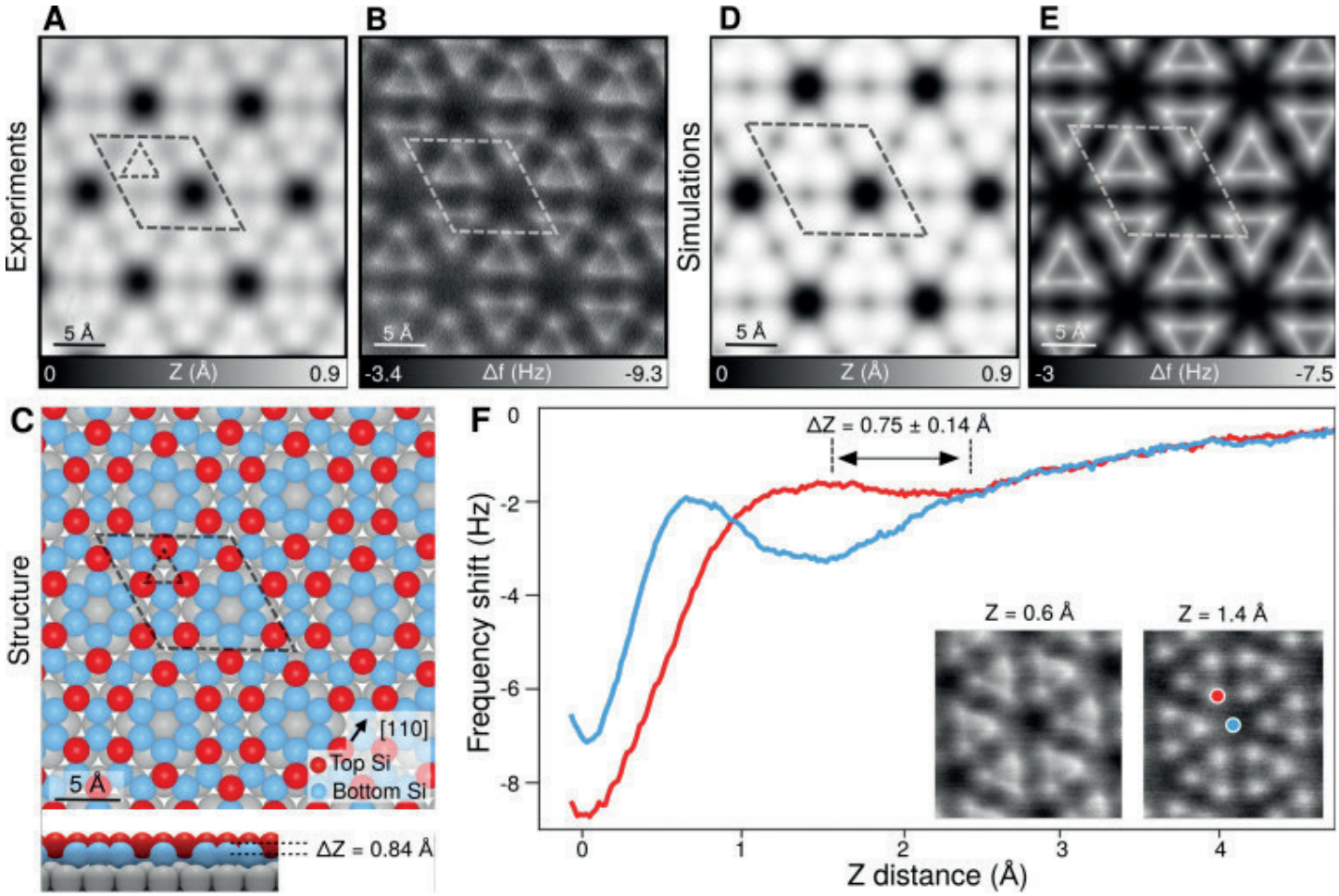

Figure 2. The 4×4 silicene lattice on Ag(111). (A and B) Experimental STM topography and constant-height AFM image acquired with CO-terminated tips at 4,5 K. (C) Representations of the 4×4 silicene structure optimized by DFT. The red and blue atoms are upmost and downmost silicon atoms of the lattice, respectively. (D and E) Simulated STM topography and AFM images from the relaxed structure. (F) Experimental force spectroscopic measurement, Δf(Z), above the 4×4 upmost (red) and downmost (blue) atoms. The vertical dashed lines show the Z positions of upmost/downmost Si atoms allowing an estimate of the buckling magnitude ΔZ. Insets are constant-height AFM images acquired at Z = 0,6 Å and Z = 1,4 Å, respectively. Reproduced from Pawlak et al. PNAS, 117, 228-237 (2020). © 2020 National Academy of Sciences.

protruding Si atoms colored in red atoms form the triangles observed in both STM/AFM images. Their side lengths are 3,86 Å while the atomic buckling obtained by comparing the upmost (red) and downmost (pale blue) Si atoms is 0.84 Å. From the calculated lattice, we computed the associated STM/AFM images (Figures 1D and E) that both indicate a good agreement with their experimental counterparts. More importantly, it allows us to identify the triangular contrast in the AFM images caused by only three upmost Si atoms in one buckled hexagonal ring. Although the 4×4 silicene lattice is a closed-packed honeycomb structure (like graphene), its intrinsic atomic buckling prevents to resolve by STM/AFM all the Si atoms of the silicene hexagons (unlike carbon rings in graphene). Thus, each triangle in the following images is associated to a buckled Si hexagonal ring.

To experimentally quantify the atomic buckling, we then performed force spectroscopic measurements above the 4×4 silicene phase. Site-dependent frequency shift curves as a function of tip – sample separation Δf(Z) were acquired above the upmost (red) and downmost (blue) Si atoms of the structure (Figure 2C and inset Figure 2F). At relative close tip – sample distances (below Z = 2,5 Å), each curve shows a “local minimum” followed by a “bump” arising from specific interactions between the front end oxygen atom of the CO-terminated tip apex and the probed Si atom of the silicene structure. The positions in Z of the dips in principle give a good estimate of the relative heights of the corresponding atoms with respect to the tip – sample distance. We extracted the upmost atoms heights as the dip position in the red curve to be Z = 2,42±0,08 Å while the lower Si atoms (blue curve) is at Z = 1.67 ± 0,05 Å. The difference of relative height ΔZ is then 0,75 Å in excellent agreement with our DFT calculations (Figure 2C) and previous results [3, 22, 32]. These observations are further confirmed by constant-height AFM images (insets of Figure 2F).

Local symmetry due to atomic buckling

Using the same strategy, the atomic buckling of the 2√3 and √13 silicene structures were characterized combining force spectroscopy and DFT calculations. By fitting the force spectroscopic curves of different atoms with a Coulomb-Buckingham potential [31], we precisely estimated the buckling magnitude in each silicene phase ranging from 0,75 ± 0,14 Å for the 4×4, 0,97 ± 0,16 Å for the 2√3 and 0,98 ± 0,32 Å for the √13. We also found out that atoms of the 2√3 and √13 phases possess three and four buckling heights in their structures, respectively. More details of the spectroscopic analysis can be found in our work [31].

Not only the relative heights of the buckled atoms is important (i.e. in the Z direction) but also their lateral positions

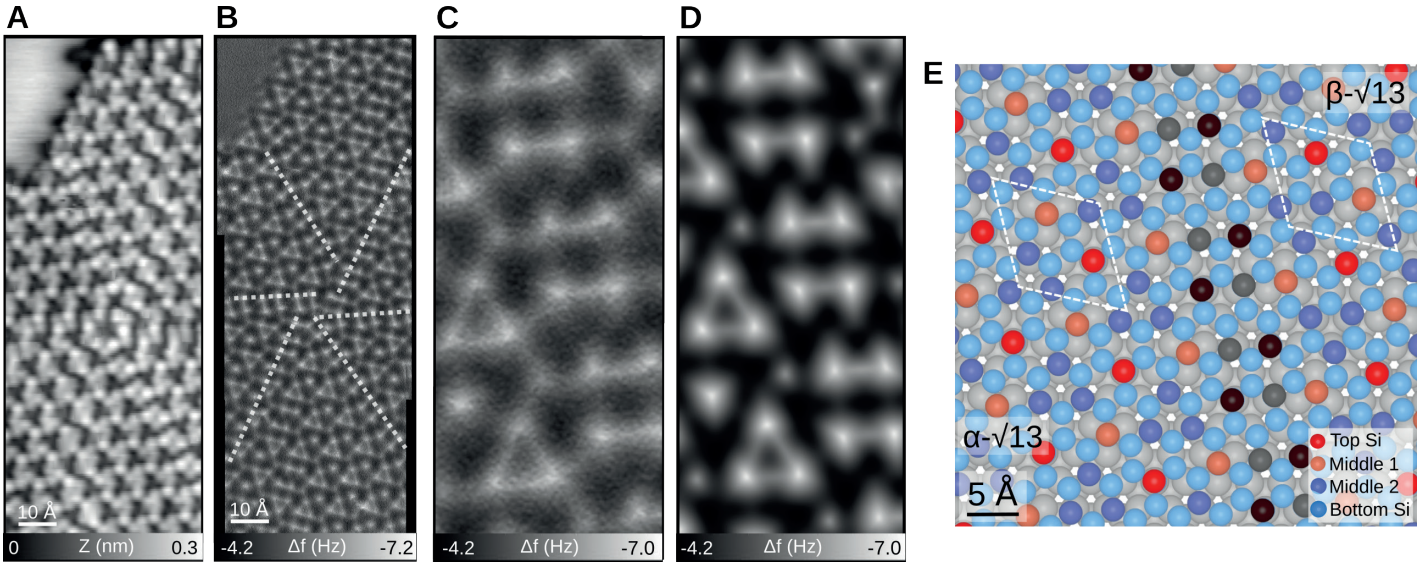

Figure 3. Local symmetry in silicene induced by variation of buckling. (A and B) Experimental STM and AFM images of the √13 moiré superstructure composed of line defects (white dashed lines) emerging from a vortex-like center. (C) Zoom-in AFM image of the line defect revealing square-like patterns and (E) Simulated AFM image obtained from the relaxed DFT structure shown in (E). According to the DFT structure, the line structure consists of a boundary between α–√13 and β–√13 chiral domains. Reproduced from Pawlak et al. PNAS, 117, 228-237 (2020). © 2020 National Academy of Sciences

within the silicene lattice. Indeed, we observed that Si atoms of similar buckling heights are precisely ordered which can lead to complex silicene restructuring. This is particularly exemplified by the √13 silicene structure (Figures 3A and B) that systematically shows vortices formed by the convergence of six defected lines (indicated by white dashed lines in Figure 3B). These boundaries separate adjacent domains of triangular features pointing in opposite directions (denoted α– and β–√13 structures as calculated by DFT of Figure 3E). Each supercell is characterized by a triangle with edges 3,6 Å long (dark blue atoms), which corresponds to a buckled Si hexagonal ring. The brighter protrusion in the AFM image of Figures 3B and C corresponds to the most protruding atom (red atom) in Figure 3E, while the second less intense bump (only observed by AFM) coincides with intermediate buckling heights (orange in Figure 3E). Despite the complexity of the pattern, the √13 lattice displays a clear *p3* symmetry with three possible rotation axes: in the triangle's epicenter as well as in either of the 2 bumps. Following symmetry arguments, we concluded to the coexistence of only two inequivalent √13 domains (i.e. α– and β–√13) that are associated by an inversion of the silicene adlayer. Energetically, the stability of these two structures is within 10 meV.

Looking now at the line defects (Figure 3C), a typical square pattern containing four maxima linked by pairs along the transversal direction. The distance between the paired atoms is 3.8 Å, thus slightly longer than the triangle sides, while the pairs are separated by 4.0 Å. Figure 3E presents the DFT relaxed structure that matches the experimental AFM image, as shown by the corresponding simulated AFM image of Figure 3D. The line defects appears to induce a large restructuring at the boundaries between the two √13 domains. However, the silicene film remains a continuous honeycomb layer without truncation and exhibits only small deformations due to a compressive strain. Note that these superstructures are stabilized on areas of several hundreds of nanometers.

Observing disordered silicene structures at domain boundaries

Interestingly, we also analyzed by AFM defected regions and boundaries between adjacent domains (Figure 4), that allow us to comment on long-standing debates of the silicene community. Indeed, previous works have reported the presence in STM images of dark regions surrounding the silicene domains which were attributed to Si-Ag alloys. Additionally, silicene domains always appear by STM topographic images embedded into the surface. These works raised numerous questions suggesting the existence of a silicon alloy instead of a true silicene adlayer. Thank to our accurate structural analysis and looking at the excellent agreement between theory and experiments, we can firmly conclude that these phases only contains Si atoms lying at

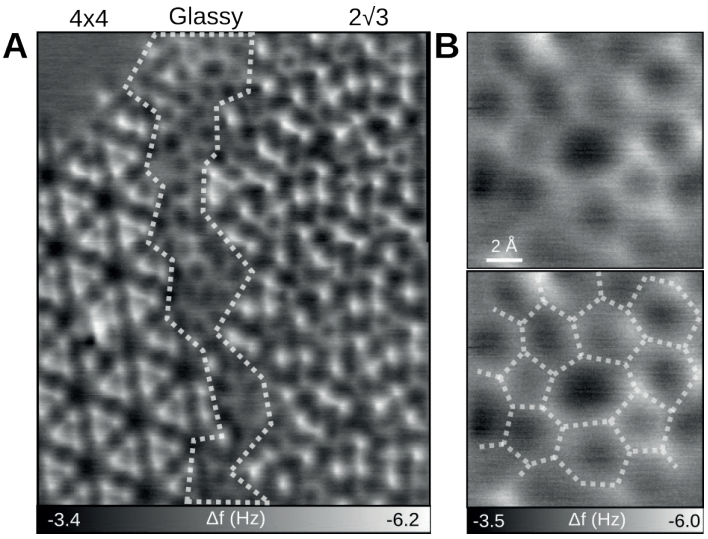

Figure 4. Imaging defects in silicene. (A) Constant-height AFM image of a grain boundary between a 4×4 and a 2√3 domain. The boundary region is delimited with white dashed lines. (B) Zoom-in AFM image of this region revealing buckled and highly distorted hexagonal, pentagonal, and heptagonal motifs (marked by white dashed lines in bottom image). Reproduced from Pawlak et al. PNAS, 117, 228-237 (2020). © 2020 National Academy of Sciences.

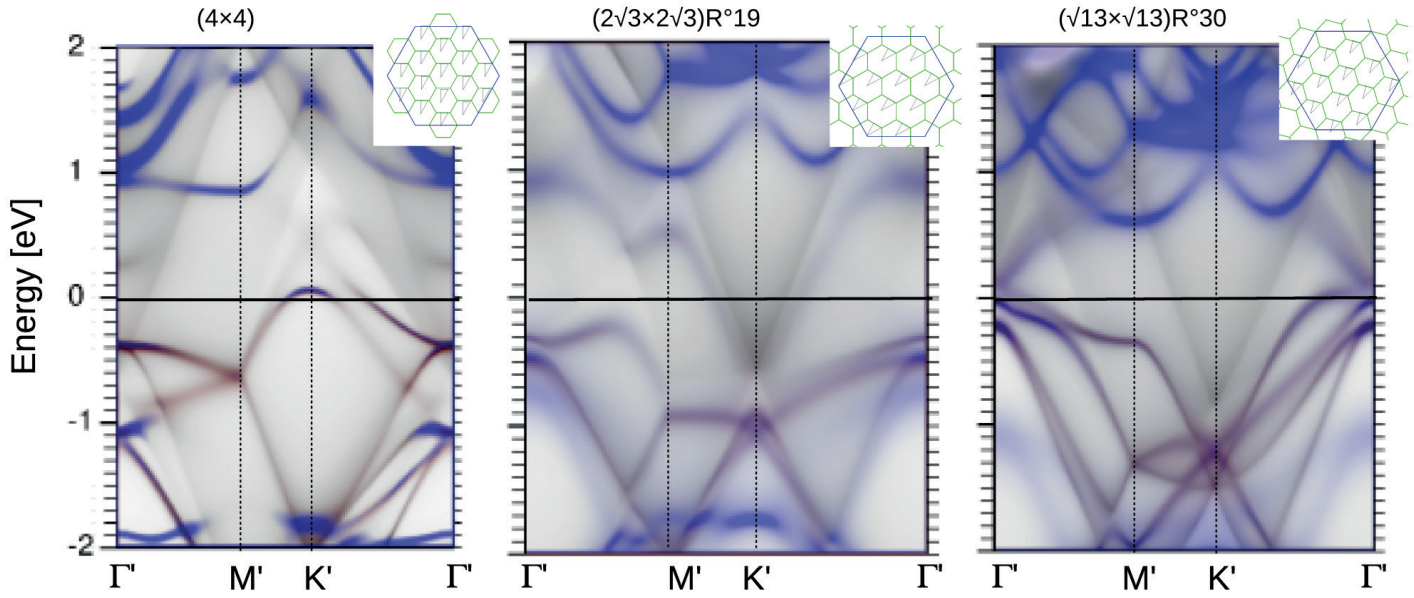

Figure 5. Calculated electronic structure of the silicene phases. (A-C), Partial density of states PDOS(k, E) projected on the surface most atoms along G0-M0-K0 for the 4×4, 2√3 and √13 silicene phases on Ag(111), respectively. Si (blue) and first Ag layer (red) projections have been superimposed on top of the second and third Ag layers (gray). Insets shows the corresponding supercells' BZ in an extended zone scheme (light green hexagons), the k-path in each case (thin solid triangles) and the Ag(111) BZ (blue). Reproduced from Pawlak et al. PNAS, 117, 228-237 (2020). © 2020 National Academy of Sciences.

0.18 Å above the silver surface [31]. Furthermore, Figure 4A shows a constant-height AFM image of a such dark STM region (white dashed line in Figure 4B) between a 4×4 and a 2√3 silicene domains on Ag(111). It reveals the signature of multiple structural motifs indicating a "glassy-like" silicene region where buckled hexagons, pentagons, and heptagons appear interconnected, in line with other Si structures where non-hexagonal motifs have been predicted [37-39].

Electronic properties of silicene on Ag(111)

From the silicene structure determined with sub-Ångstrom precision, we computed their band structure including the silver substrate (Figure 5) [31] . In each map, the projections on the Si atoms (blue) and the first Ag layer (red) have been superimposed on top of those corresponding to the subsurface Ag layers (gray). Despite the profusion of bands across the Brillouin zones (BZs) due to backfolding and apart from a few faint resonances crossing EF, all phases show a clear gap in the π bands. No sign of any Dirac cones localized within the silicene sheet appears in any of the phases, since all surface bands in the -2 to +1eV region have a strong Si-Ag1 hybridization with parabolic dispersions due to covalent bonding (in contrast with the linear metal bands). This observation is in line with previous experimental observations of silicene on Ag(111) [25, 26, 29, 30, 33-36]. We also emphasize that calculated band structures of the free-standing silicene structure phases (excluding the silver substrate) concluded the presence of Dirac cones in all the phases. Our results thus underlines, not only the pivotal role of atomic buckling in the electronic properties of silicene, but also the importance of developing novel synthesis processes or exfoliation methods towards nonconductive substrates to preserve their electronic character.

Conclusion

Our AFM/DFT-based approach is self-contained to characterize accurately the structure of silicene and other mono-element Xenes at surfaces with high lateral resolution. Importantly, local atomic bucklings can be determined with sub-Ångstrom precision independent of their structural complexity. We are thus convinced that such systematic investigation will help in foreseeing the precise structural characterization of analogous 2D materials where atomic buckling defects could lead to novel exotic properties [2].

Acknowledgment

Financial support from the Swiss National Science Foundation (SNF), the Swiss Nanoscience Institute (SNI) and the Spanish MINECO under Grant Nos. MAT2015-66888-C3-1R and RTI2018-097895-B-C41 is gratefully acknowledged. We also thank the European Research Council (ERC) under the European Union's Horizon 2020 research and innovation programme (ULTRADISS grant agreement No 834402).

References

[1] A. K. Geim & K. S. Novoselov. The rise of graphene. *Nat Mater* **6**, 183-191 (2007).
[2] A. Molle, J. Goldberger, M. Houssa, Y. Xu, S. C. Zhang & D. Akinwande. Buckled two-dimensional Xene sheets. *Nat Mater* **16**, 163-169 (2017).
[3] P. Vogt, P. D. Padova, C. Quaresima, J. Avila, E. Frantzeskakis, M. C. Asensio, A. Resta, B. Ealet & G. L. Lay. Silicene: compelling experimental evidence for graphene like two-dimensional silicon. *Phys. Rev. Lett* **108**, 155501 (2012).
[4] M. E. Dávila, L. Xian, S. Cahangirov, A. Rubio & G. L. Lay. Germanene: a novel two-dimensional germanium allotrope akin to graphene and silicene. *New J Phys* **16**, 095002 (2014).
[5] F. F. Zhu, W.-J. Chen, Y. Xu, C.-L. Gao, D.-D. Guan, C.-H. Liu, D. Qian, S.-C. Zhang & J.-F. Jia. Epitaxial growth of two-dimensional stanene. *Nat. Mater.* **14**, 1020-1025 (2015).
[6] G. Bihlmayer, J. Sassmannshausen, A. Kubetzka, S. Blügel, K. von Bergmann & R. Wiesendanger. Plumbene on a Magnetic Substrate: A Combined Scanning Tunneling Microscopy and Density Functional Theory Study. *Phys. Rev. Lett* **124**, 126401 (2020).
[7] C.-C. Liu, W. Feng & Y. Yao. Quantum spin Hall effect in silicene and two-dimensional germanium. *Phys. Rev. Lett* **107**, 076802 (2011).
[8] M. Ezawa. Topological insulators in silicene: Quantum hall, quantum spin hall and quantum anomalous hall effects. *AIP Conference Proceedings* **1566**, 199 (2013).
[9] F. e. a. Reis. Bismuthene on a SiC substrate: A candidate for a high-temperature quantum spin Hall material. *Science* **357**, 287- 290 (2017).

[10] Z.-Q. Huang, C.-H. Hsu, F.-C. Chuang, Y.-T. Liu, H. Lin, W.-S. Su, V. Ozolins & A. Bansil. Strain driven topological phase transitions in atomically thin films of group IV and V elements in the honeycomb structures. *New Journal of Physics* **16,** 105018 (2014).
[11] L. Gross, F. Mohn, N. Moll, P. Liljeroth & G. Meyer. The chemical structure of a molecule resolved by atomic force microscopy. *Science* **325**, 1110-1114 (2009).
[12] L. Gross. Recent advances in submolecular resolution with scanning probe microscopy. *Nature Chemistry* **3**, 273-278 (2011).
[13] R. Pawlak, S. Kawai, S. Fremy, T. Glatzel & E. Meyer. Atomic-Scale Mechanical Properties of Orientated C_{60} Molecules Revealed by Noncontact Atomic Force Microscopy. *ACS Nano* **5**, 6349-6354 (2011).
[14] S. Kawai, A. Sadeghi, T. Okamoto, C. Mitsui, R. Pawlak, T. Meier, J. Takeya, S. Goedecker & E. Meyer. Organometallic Bonding in an Ullmann-Type On-Surface Chemical Reaction Studied by High-Resolution Atomic Force Microscopy. *Small* **12**, 5303-5311 (2016).
[15] S. Kawai, V. Haapasilta, B. D. Lindner, K. Tahara, P. Spijker, J. A. Buitendijk, R. Pawlak, T. Meier, Y. Tobe, A. S. Foster & E. Meyer. Thermal control of sequential on-surface transformation of a hydrocarbon molecule on a copper surface. *Nature Communications* **7**, 12711 (2016).
[16] P. Ruffieux, S. Wang, B. Yang, C. Sánchez-Sánchez, J. Liu, T. Dienel, L. Talirz, P. Shinde, C. A. Pignedoli, D. Passerone, T. Dumslaff, X. Feng, K. Müllen & R. Fasel. On-surface synthesis of graphene nanoribbons with zigzag edge topology. *Nature* **531**, 489-492 (2016).
[17] S. Kawai, S. Nakatsuka, T. Hatakeyama, R. Pawlak, T. Meier, J. Tracey, E. Meyer & A. S. Foster. Multiple heteroatom substitution to graphene nanoribbon. *Sci Adv* **4**, eaar7181 (2018).
[18] S. Mishra, D. Beyer, K. Eimre, S. Kezilebieke, R. Berger, O. Gröning, C. A. Pignedoli, K. Müllen, P. Liljeroth, P. Ruffieux, X. Feng & R. Fasel. Topological frustration induces unconventional magnetism in a nanographene. *Nature Nanotechnology* **15**, 22-28 (2020).
[19] Y. Sugimoto, P. Pou, M. Abe, P. Jelinek, R. Pérez, S. Morita & O. Custance. Chemical identification of individual surface atoms by atomic force microscopy. *Nature* **446**, 64-67 (2007).
[20] B. Feng, B. Feng, Z. Ding, S. Meng, Y. Yao, X. He, P. Cheng, L. Chen & K. Wu. Evidence of Silicene in Honeycomb Structures of Silicon on Ag(111). *Nano Lett* **12**, 3507 (2012).
[21] L. Chen, C. Liu, B. Feng, X. He, P. Cheng, Z. Ding, S. Meng, Y. Yao & K. Wu. Evidence for Dirac Fermions in a Honeycomb Lattice Based on Silicon. *Phys. Rev. Lett* **109**, 056804 (2012).
[22] C.-L. Lin, R. Arafune, K. Kawahara, N. Tsukahara, E. Minamitani, Y. Kim, N. Takagi & M. Kawai. Structure of Silicene Grown on Ag(111). Appl. Phys. Exp 5, 045802 (2012).
[23] H. Jamgotchian, Y. Colignon, N. Hamzaoui, B. Ealet, J. Y. Hoarau, B. Aufray & J. P. Bibérian. Growth of silicene layers on Ag(111): unexpected effect of the substrate temperature. *J. Phys.: Cond. Matt* **24**, 17 (2012).
[24] R. Arafune, K. K. C.-L. Lin, N. Tsukahara, E. Minamitani, Y. Kim, N. Takagi & M. Kawai. Structural transition of silicene on Ag(111). *Surf. Science* **608**, 297 (2013).
[25] D. Tsoutsou, E. Xenogiannopoulou, E. Golias, P. Tsipas & A. Dimoulas. Evidence for hybrid surface metallic band in (4×4) silicene on Ag(111). *Appl. Phys. Lett* **103**, 231604 (2013).
[26] Y. Feng, D. Liu & B. Feng. Direct evidence of interaction-induced Dirac cones in a monolayer silicene/Ag(111) system. *Proc. Natl. Acad. Sci. USA*, (2016).
[27] P. M. Sheverdyaeva, P. M. Sheverdyaeva, S. K. Mahatha, P. Moras, L. Petaccia, G. Fratesi, G. Onida & C. Carbone. Electronic States of Silicene Allotropes on Ag(111). *ACS Nano* **11**, 975 (2017).
[28] H. Enriquez, S. Vizzini, A. Kara, B. Lalmi & H. Oughaddou. Silicene structures on silver surfaces. *J. Phys.: Condens. Matter* **24**, 314211 (2012).
[29] Z.-X. Guo, S. Furuya, J.-I. Iwata & A. Oshiyama. Absence of Dirac Electrons in Silicene on Ag(111) Surfaces. *J. Phys. Soc. Japan* **82**, 6 (2013).
[30] E. Scalise, M. Houssa, G. Pourtois, B. van den Broek, V. Afanas'ev & A. Stesmans. Vibrational properties of silicene and germanene. *Nano Research* **6**, 19-28 (2013).
[31] R. Pawlak, C. Drechsel, P. D'Astolfo, M. Kisiel, E. Meyer & J. I. Cerda. Quantitative determination of atomic buckling of silicene by atomic force microscopy. *Proc Natl Acad Sci USA* **117**, 228 (2020).
[32] A. Curcella, R. Bernard, Y. Borensztein, A. Resta, M. Lazzeri & G. Prevot. Determining the atomic structure of the (4 × 4) silicene layer on Ag(111) by combined grazing-incidence x-ray diffraction measurements and first-principles calculations. *Phys Rev B* **94**, 165438 (2016).
[33] J. Sone, T. Yamagami, Y. Aoki, K. N. &. H. Hirayama. Epitaxial growth of silicene on ultra-thin Ag(111) films. *New J. Phys* **16**, 095004 (2014).
[34] G. Prévot, R. Bernard, H. Cruguel & Y. Borensztein. Monitoring Si growth on Ag(111) with scanning tunneling microscopy reveals that silicene structure involves silver atoms. *App. Phys. Lett* **405**, 213106 (2014).
[35] Y. Borensztein, A. Curcella, S. Royer & G. Prévot. Silicene multilayers on Ag(111) display a cubic diamondlike structure and a 3×3 reconstruction induced by surfactant Ag atoms. *Phys. Rev. B* **92**, 155407 (2015).
[36] R. Bernard, Y. Borensztein, H. Cruguel, M. Lazzeri & G. Prévot. Growth mechanism of silicene on Ag(111) determined by scanning tunneling microscopy measurements and ab initio calculations. *Phys. Rev. B* **92**, 045415 (2015).
[37] S. Li, Y. Wu, Y. Tu, Y. Wang, T. Jiang, W. Liu & Y. Zhao. Defects in Silicene: Vacancy Clusters, Extended Line Defects, and Di-adatoms. *Sci. Rep* **5**, 7881 (2015).
[38] D. Ghosh, P. Parida & S. K. Pati. Stable line defects in silicene. *Phys. Rev. B* **92**, 195136 (2015).
[39] J. I. Cerdá, J. Sławińska, G. L. Lay, A. C. Marele, J. M. Gómez- Rodríguez & M. E. Dávila. Unveiling the pentagonal nature of perfectly aligned single-and double-strand Si nanoribbons on Ag(110). *Nat. Comm* **7**, 13076 (2016).

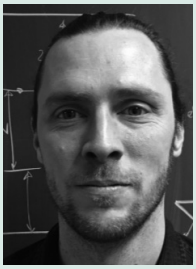

Rémy Pawlak has been a senior scientist at the University of Basel since 2017 in the group of Prof. Dr. E. Meyer, that he joined as postdoctoral fellowship in 2010. He is working on atomic and molecular characterization and their manipulation by scanning tunneling microscopy (STM) and atomic force microscopy (AFM) in cryogenic environment. He studied at the Aix-Marseille University, where he received his PhD in Physics and nanosciences in 2010 for the growth of supramolecular and polymerized molecular networks at surfaces studied by STM/AFM.

Ernst Meyer is professor of physics at the University of Basel since 1997. His main interests are nanomechanics experiments with a focus on atomic friction and energy dissipation. The transition from metallic to superconductive phase was observed by non-contact friction experiments. High resolution force microscopy is an important tool to characterize surfaces or molecular aggregates. Experiments with graphene nanoribbons and metallic nanowires were performed to get further insight into the mechanical, electrical and magnetic properties of these assemblies.

Jorge Iribas Cerdá is a staff senior researcher at Materials Science Institute of Madrid (ICMM-CSIC) since 2012. His main research interest is the theoretical understanding of surface and interface properties from DFT and post-DFT formalisms, some of them developed and implemented by himself along the last two decades. He counts with a long expertise in the simulation of STM images explicitly including the tip apex; a tool that has allowed the resolution of a number of complex surface structures. Currently he is intensely involved in spin-orbit related phenomena.